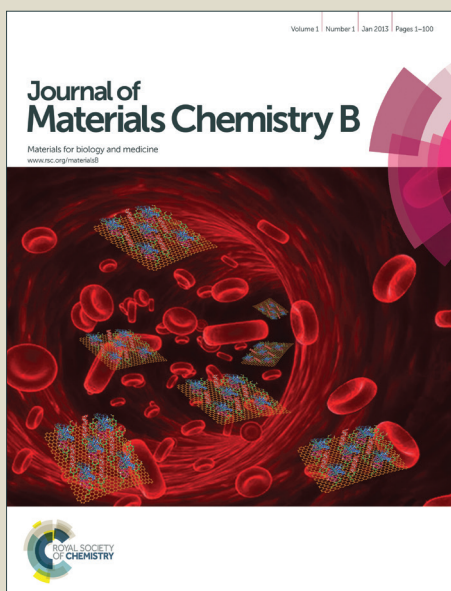


Journal of Materials Chemistry B

Accepted Manuscript



This is an *Accepted Manuscript*, which has been through the Royal Society of Chemistry peer review process and has been accepted for publication.

Accepted Manuscripts are published online shortly after acceptance, before technical editing, formatting and proof reading. Using this free service, authors can make their results available to the community, in citable form, before we publish the edited article. We will replace this *Accepted Manuscript* with the edited and formatted *Advance Article* as soon as it is available.

You can find more information about *Accepted Manuscripts* in the [Information for Authors](#).

Please note that technical editing may introduce minor changes to the text and/or graphics, which may alter content. The journal's standard [Terms & Conditions](#) and the [Ethical guidelines](#) still apply. In no event shall the Royal Society of Chemistry be held responsible for any errors or omissions in this *Accepted Manuscript* or any consequences arising from the use of any information it contains.

ARTICLE

Silica@proton-alginate microreactors: a versatile platform for cell encapsulation

Cite this: DOI: 10.1039/x0xx00000x

Cecilia Spedalieri,^a Clémence Sicard,^{b,c} Mercedes Perullini,^a Roberta Brayner,^c Thibaud Coradin,^b Jacques Livage,^b Sara A. Bilmes^a and Matías Jobbágy^{*a}.Received 00th January 2012,
Accepted 00th January 2012

DOI: 10.1039/x0xx00000x

www.rsc.org/

As an alternative approach to the well known Ca(II)-Alginate encapsulation process within silica hydrogels, proton-driven alginate gelation was investigated in order to establish its capacity as a culture carrier, both isolated and embedded in an inorganic matrix. Control over the velocity of the proton-gelation front allows the formation of a hydrogel shell while the core remains liquid, allowing bacteria and microalgae to survive the strongly acidic encapsulation process. Once inside the inorganic host, synthesized by a sol-gel process, the capsules spontaneously redissolve without the aid of external complexing agents. The entrapped cells survive the two-step process in a significant extent; culture's growth restores the initial cell count in less than two weeks. Biosynthesis of Au nanoparticles mediated by the entrapped microalgae illustrates the preservation of the biosynthetic abilities supported by this platform.

Introduction

Alginate-based hydrogels offer a universal platform for the preparation of biomaterials, ranging from macroscopic scaffolds¹ to micrometric capsules^{2,3} hosting enzymatic and/or cellular activity.⁴⁻⁶ The structure of this biopolymer is based on linear copolymers that contain homopolymeric blocks of (1,4)-linked β -D-mannuronic acid (M) and its C-5 epimer, α -L-guluronic acid (G) residues. These units are covalently linked together in different sequences or blocks composed by the same unit (MMMM or GGGGG) or alternating them (GMGMGM); their relative amount and monomer distribution depends on the origin of alginate.⁷ Typically, the consolidation of these macromolecules in the form of hydrogels lies on the ability of alginate carboxylates to crosslink its chains by Me(II) complexation, giving rise to Me(II)-Alg hydrogels. Among cations, divalent ones as Ca(II) or transition metal ones and trivalent rare earths can easily drive the process.⁸⁻¹² Monovalent cations such as potassium can also interact with the polymer chains forming a hydrogel.¹³⁻¹⁶ In the case of calcium, the procedure can take place under mild pH conditions, allowing the quantitative entrapment of cell cultures suspended in sodium-alginate solutions (Na-Alg) ensuring as well long-term viability once entrapped in the Ca-Alg hydrogel.¹⁷ Depending on their inherent toxicity, other divalent or trivalent cations can be employed in/ for biologically active species encapsulation process.

For certain applications, these cross-linked alginate phases are employed as culture carriers to be included within a stable matrix, including polymer scaffolds,¹⁸ carbon nanotube-based assemblies¹⁹ and microporous silica hydrogels.²⁰ Once entrapped within a stable hydrogel or scaffold, the cross-linked alginate phase can be liquefied by means of citrate-driven Ca(II) sequestration. The former Ca-Alg hydrogel gives rise to liquid voids within the silica hydrogels; inside these voids,

cultures can grow isolated from the outer liquid media. Then, these culture growth platforms can prevent contamination with foreign strains, while nutrient can diffuse through the hydrogel in a proper period of time, allowing calli growth,¹⁷ biosensing,²¹ biodegradation,²² etc.

As an alternative approach, the Na-Alg solution can be gelled through the addition of acids. Once a critical fraction of carboxylate residues are protonated, the decrease in the polymer charge density allows for chain-chain interactions leading to gelation. The inherent pH for the consolidation of H-Alg hydrogel is around 3.5, depending on the mannuronic ($pK_a = 3.38$) to guluronic acid ($pK_a = 3.65$) relative content of the employed alginate.²³ However, H-Alginate being intrinsically an aggressive matrix, it is not surprising that its use as a culture carrier was not reported so far. Interestingly, while Ca(II) driven gelation can be mildly reverted by mean of biocompatible sequestration with citrate, proton-driven one can be reverted with a moderate biocompatible pH rise. The present work introduces the application of this approach as a straight and faster alternative procedure for the preparation of biologically active alginate carriers entrapped within silica hydrogels. The survival of microalgae within these hybrid platforms is demonstrated and the preservation of their biosynthetic abilities is illustrated by means of the biosynthesis of Au nanoparticles.

Experimental Section

Alginate. 1. Sodium alginate (from Brown Algae, Sigma), $\text{HAuCl}_4 \cdot 3\text{H}_2\text{O}$ (Acros Organics), $\text{CaCl}_2 \cdot 2\text{H}_2\text{O}$ (Sigma) and HCl (Merck) were used as received. Solutions of sodium alginate 2 or 3% wt. were prepared by dissolving the proper amount of the polysaccharide in Milli-Q® water and left under stirring overnight prior to use. 2. Afterwards, the alginate solution was put in contact with a solution of crosslinking cation in an arrangement according to

the required experimental measurement. Crosslinked samples were named Ca-Alg, H-Alg, according to the cation that drives alginate gelation. **3.** For the titration curve, known masses of sodium alginate 2% were left overnight with different amounts of HCl 0.1 M and MilliQ water. Equilibrium pH was then measured in the liquid phase and plotted against the HCl mass added.

Culture growth and purification. 1. *Escherichia coli* cultures used in this work were grown in Tryptone Soy Medium (TS) overnight at 37°C. Prior to addition to the alginate solution, cultures were centrifuged to obtain concentrated pellets. **2.** *Chlorella vulgaris* cultures used in this work were grown in Bold's Basal Medium (BBM) enriched with vitamins (Thiamine -B1-, Cobalamine -B12-, Biotin; conc. 1×10^{-5} M). Temperature was maintained at $20 \pm 2^\circ\text{C}$, with illumination alternating between 16 h light and 8 h darkness. Prior to addition to the alginate solution, algae culture was centrifuged to obtain concentrated pellets.

Alginate gel preparation, characterization and culture encapsulation. 1. To obtain beads, the alginate solution was added dropwise to stirred solutions of HAuCl_4 , CaCl_2 or HCl (concentrations between 0.1 M to 0.01 M) at a constant velocity with a syringe needle. **2.** A suspension of *E. coli* in alginate 2% and 3% (10^9 CFU/mL) was added dropwise to an HCl 0.06 M solution. The formed beads were extracted at different times and left in phosphate buffer until dissolution. Afterwards, serial dilutions were grown in solid TS-Agar medium for CFU count. **4.** A suspension of *C. vulgaris* in alginate 2% and 3% (10^6 cells/mL) was added dropwise to an HCl 0.06M solution. After 1 minute, the formed beads were extracted and left in an excess of sterile water until encapsulation. When encapsulating with Ca-Alg, alginate was added dropwise to a CaCl_2 0.01 M solution and left stirring for 10 minutes. Beads were extracted after the mentioned time and left in an excess of sterile water until encapsulation.

Silica hydrogel encapsulation. 1. Tetraethoxysilane alcohol-free route (TAFR) silica hydrogels: silica sol was made by mixing 20 mL of tetraethoxysilane (TEOS 98%), 6.25 mL of H_2O and 0.72 mL of HCl 0.6 M. The sol was vigorously stirred for 24 h. To obtain the aqueous sol, the hydrolyzed silica sol was diluted with an equal volume of H_2O , and ethanol removed from this mixture under vacuum (40°C , 30 mbar) until the weight loss equaled that of ethanol generated by the hydrolysis reaction. The silica-based gels were obtained by mixing the aqueous silica sol and phosphate buffer solution (0.2 M, pH 7.0). Volumes of silica sol and water were varied to obtain 3.6, 5.4, 7.2, 9 and 10.7 % wt SiO_2 in the final hydrogel.^{24, 25} **2.** Silicate/Ludox® (SL) hydrogels: appropriate volumes of 2 M sodium silicate, commercial colloid silica (Ludox HS-40), phosphate buffer solution (0.2 M, pH 7.0), Milli-Q® water and small amounts of HCl 4 M (when needed) were mixed in order to obtain varying proportions of polymeric to particulate silica precursors (1:3, 1:4 and 1:5) and 10.7% SiO_2 in the final hydrogel.^{20, 26} **3.** Optical properties of TAFR and SL hydrogels were evaluated by attenuation at different wavelengths immediately after complete gelation, with particular interest in the 650-750 nm wavelength interval. **4.** For the encapsulation process, TAFR and SL gels were prepared as previously described and, immediately after mixing the reactants, the beads are added. For algae cell counting, a Neubauer chamber was used.

Proton/Au(III) diffusion, uptake and reduction. 1. In order to assess the inherent interaction of Na-Alg solution with HAuCl_4 solutions, diffusion experiments were carried out in PMMA 1.5 mL cuvettes. In a typical experiment, 1 mL of Na-Alg solution was placed in a cuvette with a small piece of dialysis membrane on top to ensure a planar diffusion front. 500 μL of HAuCl_4 and HCl solutions was added, and the cuvettes immediately placed on a digital scanner. When analysing proton diffusion, acid-base indicators were added to the alginate and the HCl solution. To guarantee a robust analysis, two different gold concentrations were used, and four proton concentrations: two with the same pH as the Au(III) solutions, and two with the same charge equivalents as the Au(III) solutions. Images were acquired with a scanner at regular periods of time, and analyzed with ImageJ free software to obtain profiles of colour intensity. **2.** The concentration of Au(III) in the alginate beads was performed by ICP analysis. 2% and 3% alginate beads were left in HAuCl_4 0.01M for different times (10, 20, 30 and 60 min) and they dissolved in concentrated HCl for further analysis. **3.** The characteristics of the interaction between alginate and the crosslinking cation were explored by means of ATR-FTIR spectroscopy, employing FTIR Nicolet 8700 equipped with a diamond crystal sample holder. Alginate cylindrical shapes were obtained by filling wells of 96-well microplaque with 300 μL of alginate solution, and slowly adding concentrated crosslinking cation solution on top to ensure complete crosslinking. All samples were measured as made. These conformations were used to ensure proper contact between the samples and the diamond crystal.

Au nanoparticle characterization. 1. Characterization of nanoparticles was made by scanning electron microscopy (FESEM Zeiss Supra-40) equipped with energy dispersive X-ray spectroscopy (EDS) probe, UV-visible spectroscopy (Ocean Optics) and powder X-ray diffraction (Siemens D5000) using graphite filtered Cu K α radiation ($\lambda = 1.5406 \text{ \AA}$), with a 0.05 degrees step size and 15 s step time.

Results and discussion

The formation of proton cross-linked alginate gels, H-Alg in the following, was investigated both by equilibrium and kinetic determinations. The former was assessed by acid titration, confirming a gelation pH in the range 3.0-4.0, while the latter was inspected by straight observation of digital images acquired from the gelation process.²⁷ Figure 1 presents digital images of the H-Alg phase evolution, driven by HCl diffusion in the presence of Methyl Orange and Methyl Red acid-base indicators; their pH range of color transition are 3.1-4.4 and 4.4-6.2, respectively. These observations as well as others performed with other indicators revealed that the pH of gelation front lies below 4.4 (see ESI, Figure S1). Under the explored conditions, the H-Alg phase gelation front develops at a rate of *ca.* 4 mm h⁻¹.

Journal Name

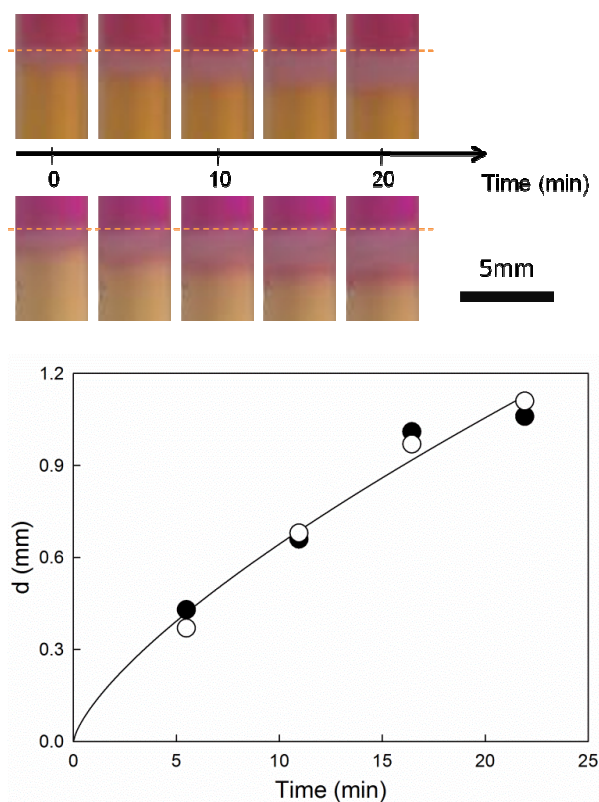


Figure 1. Upper panel: digital images of proton (HCl 0.17M) diffusion profiles in Na-Alg 3% wt, followed with Methyl Orange (pH 3.1-4.4; up) and Methyl Red (pH 4.4-6.2; down); dotted orange line depict the limit between the upper HCl reservoir and the lower alginate gel/solution. Lower panel: evolution H-Alg gel thickness for Na-Alg 3 wt% solutions containing Methyl Orange (filled circles) and Methyl Red (empty circles).

From the aforementioned results, it can be concluded that the use of fully gelled H-Alg would be restricted for culture entrapment of strains that remain viable at pH values lower than 4.4. However, when alginate gels are prepared in the form of beads, it is possible to imagine the formation of an H-Alg shell that could ensure the bead integrity and culture isolation from the outer liquid media and would coexist with a remnant liquid inner core retaining a non acid condition and hence preserving a fraction of the starting culture viable for a suitable period of time. The success of this approach relies on the control of proton cross-linking front. In order to demonstrate the feasibility of this procedure, a suspension of *E. coli* grown overnight was centrifuged to concentrate the culture as a pellet that was redispersed in Na-Alg 2% and 3% solutions until homogeneity. Then, these suspensions were added drop wise to a solution of HCl 0.06 M (to trigger gelation), and left immersed for increasing times (0-4 min). Once extracted, the beads were transferred to 1 mL phosphate buffer 0.1 M (pH 7.2) and left until total redissolution (10-15 min); serial dilutions were made of each sample and left to grow in agar-TS for CFU count. For cells suspended in 2% alginate viability decreases below 50% after 2 min, and after 4 min it decreases dramatically. However, higher concentrations of alginate allow better results after short periods due to the inherently higher buffer capacity of the biopolymer.

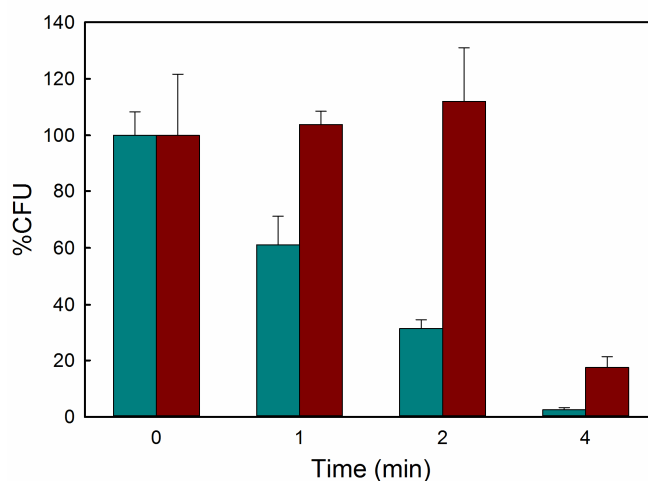
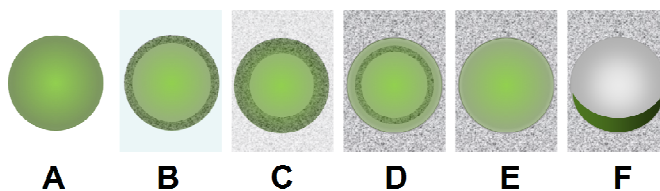


Figure 2. Viability of *E. coli* encapsulated in H-Alginate 2% (up) or 3% (down) as a function of time.

Therefore, a two minutes-long time window guarantees viable conditions for the inner fraction of the culture, allowing its coupling with the second step (entrapment within a silica hydrogel). The latter phase formation is driven by sol-gel silica polymerization at neutral pH conditions in less than a minute due to the addition of phosphate buffer. In parallel with this process, the neutral buffer can diffuse towards the alginate bead, driving the liquefaction of alginate and restoring a cytocompatible pH within the whole void (see Scheme 1).



Scheme 1. (A) Starting Na-Alg drop loaded with the suspended *C. vulgaris* culture. (B) Immersion in acid solution and birth of H-Alg rigid shell (opaque layer) around Na-Alg liquid core through the diffusion of protons from the outer acid media. (C) Growth of the H-Alg shell towards the liquid centre of the bead (viable culture) immersed in an acid solution of silica precursors. (D) Sol-gel transition driven by addition of buffer solution to the silica precursors; partial liquefaction of the H-Alg shell through the diffusion of protons towards the outer buffered media. (E) Silica hydrogel consolidation and total liquefaction of the H-Alg shell creating a liquid void. (F) Decantation of *C. vulgaris* culture inside the liquid void.

The aforementioned concept was demonstrated entrapping *C. vulgaris* microalgae within alkoxide-based SiO_2 (TAFR) hydrogels of high optical quality. The procedure easily gives rise to liquid voids within silica hydrogel. Figure 3 depicts images of culture-loaded beads just after entrapment within the silica hydrogel and after a 48 h-long aging. A close up of H-Alg beads reveals a pale green shell, corresponding to steps B-D depicted in Scheme 1. Cultures contained within Ca-Alg beads (control) remain fixed in a rigid hydrogel, while those formerly occupied by H-Alg were able to decant due to the liquid nature of the voids. These high optical quality hydrogels (see ESI, Figure S2) loaded with viable cultures constitutes a very promising biosensing platform²⁸⁻³⁰ among other applications.³¹

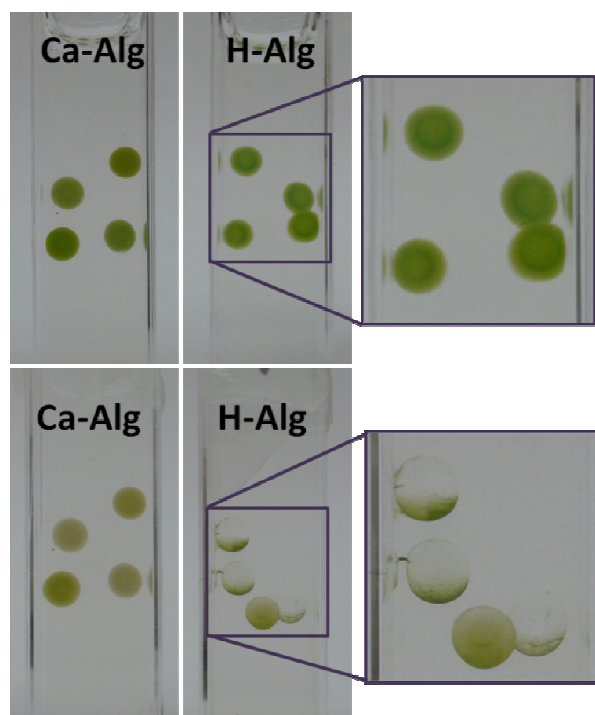


Figure 3. Silica TAFR hydrogels (10.7% SiO₂) containing *C. vulgaris*-loaded Ca-Alg and H-Alg beads immediately after gelation (upper image) and after 48 h (lower image). Inset: detail of re-liquefied H-Alginate voids.

Beyond their potential role as sensing platforms, SiO₂-hydrogels hosting *C. vulgaris* cultures were demonstrated to be effective bioreactors for the biosynthesis of metallic nanoparticles.³² In that scenario, aqueous silica-based (SL) hydrogels are preferred for being less expensive and more reproducible, allowing an easy scale up, even though their lower optical quality. Several formulations hosting *C. vulgaris* were tested in mid-term period. Figure 4 presents the cell count of *C. vulgaris* (percentage respect to initial alginate bead) after two weeks entrapped in varied SL gels using H-Alg and control Ca-Alg hydrogels. Only deep green cells were taken into account in order to properly reflect the fraction of photosynthetically active cells. An optical inspection of the whole encapsulated culture as performed with was not possible in this case due to the inherent opacity of SL gel. It is worth mentioning that *C. vulgaris* cell count after 1 min encapsulation within 2 and 3% Ca and H-alginate resulted in no depletion, in contrast with *E. coli* behaviour (Figure 2). All the formulations revealed a suitable level of viability, compensating the initial loss due to Alg acidification with cellular growth within the voids. As a result, after two weeks, the cell population was similar (Alg 3%) if not higher (Alg 2%) for H-Alg beads compared to Ca-Alg.

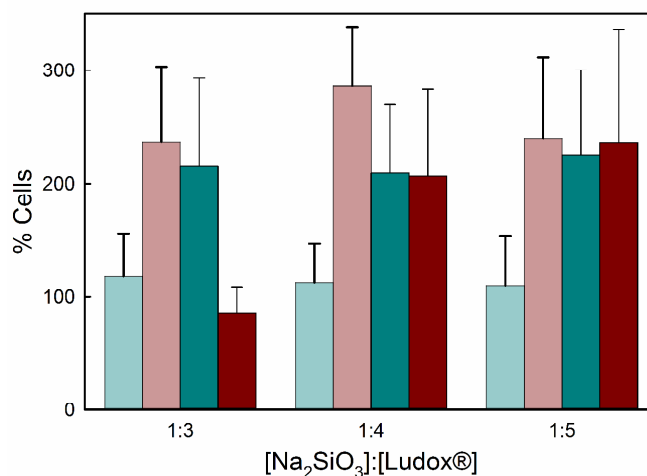


Figure 4. *C. vulgaris* cell count (percentage respect to initial alginate bead) after two weeks entrapped in 2% (blue) or 3% (red) alginate crosslinked with calcium (light colour) or protons (intense colour) dispersed within SL (Silicate:Ludox[®] 1:3, 1:4 or 1:5) hydrogels.

Once confirmed the suitability of SL hydrogels to entrap *C. vulgaris*, their ability to perform biosynthesis of Au nanoparticles was tested. To this aim a cuvette loaded with 1:3 hydrogel containing a single H-Alg (2%) bead was exposed to an external solution of HAuCl₄ 0.02 M, in order to reach a final concentration of 10⁻³ M. This concentration was chosen as compromise of reaction yield while preventing spontaneous Au(III) reduction driven by alginate, as observed for higher HAuCl₄ concentrations (see ESI, Figure S4). Yellow colour of Au(III) precursor was noticed within the SL hydrogel, even beyond the zone of the entrapped culture, confirming the absence of spontaneous reduction within the SL hydrogel support. Control experiments prepared without loading the culture reveal no significant reduction either within SL hydrogel nor inside the H-Alg cavity (see ESI, Figure S3-S5). The eventual stabilization of Au(III) ions in the form of an Au(III) cross-linked alginate hydrogel³³ could be disregarded; FTIR analysis of samples prepared exposing Na-Alg to HAuCl₄ solutions revealed the main features observed for bare H-Alg control (See Figure 5). In addition once washed with water, soluble Au(III) was released, leaving a stable H-Alg hydrogel (see ESI, Figure S7).

Once the reagent diffused through the SL hydrogel and reached the *C. vulgaris* liquid culture (4 h), Au(III) reduction was noticed by the appearance of the pink-purple colour inherent to plasmonic absorption band of nanometer-size metallic gold (see Figure 6).

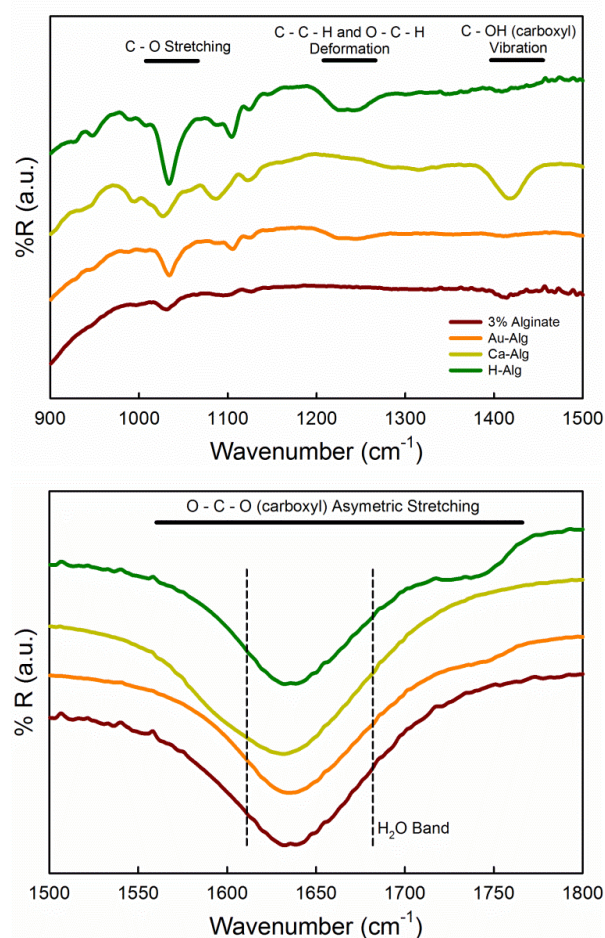


Figure 5. ATR-FTIR spectra recorded on Na-Alg 3% solution and representative alginate hydrogels.

FESEM images of *C. vulgaris* extracted from the bioreactor after 30 h denoted the presence of a dense deposit of nanoparticles on their external surface; EDS elemental mapping confirmed an homogenous signal of Au. An extract of redispersed particles revealed the characteristic diffraction lines of crystalline metallic gold; UV-Vis spectroscopy evidenced a marked absorption maximum ascribable to the plasmonic resonance band of nanometric metallic gold (see ESI, Figure S9). Similar results were observed once the experiment was repeated employing H-Alg (3%), in good agreement with viability screening results.

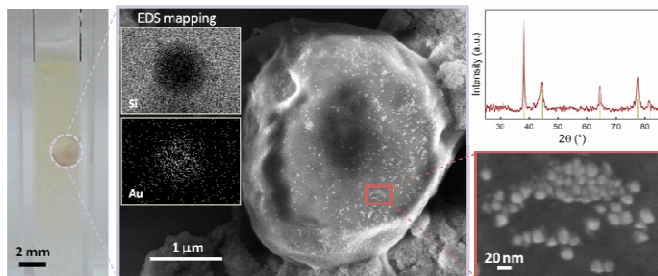


Figure 6. SL hydrogel loaded with a *C. vulgaris* culture (7×10^4 CFU/mL) in H-Alg 3% exposed to HAuCl_4 10^{-3} M for 24 h.

Conclusions

Proton-driven alginate gelation offers a fast and reversible path for the preparation of isolated liquid cultures entrapped within silica hydrogels. Despite the aggressive pH imposed by H-Alg consolidation, a significant fraction of the culture entrapped within the alginate capsule remains under viable conditions; after liquefaction culture growth can restore or even increase the starting count, preserving its biosynthetic abilities. The microalgae-assisted preparation of Au nanoparticles demonstrates the possibility for an external feed of reagents and confinement of resulting products in a small volume, allowing their easy extraction and purification from reaction media.

Acknowledgements

This work was performed in the frame of the ECOS-Sud PA07E08 program and has been supported by the University of Buenos Aires (UBACyT 20020130100048BA), the National Agency for Science and Technology Promotion of Argentina (PICT-2012-1167) and the National Research Council of Argentina (CONICET PIP 11220110101020). MP, SAB and MJ are Researchers of CONICET (Argentina). CS thanks MQ for software development and support.

Notes and references

^a Laboratorio de Superficies y Materiales Funcionales INQUIMAE-DQIAQF, Facultad de Ciencias Exactas y Naturales, Universidad de Buenos Aires, Ciudad Universitaria Pab. II, C1428EHA, Buenos Aires (Argentina). E-mail: jobbag@qi.fcen.uba.ar.

^b UPMC Univ Paris 06, CNRS, UMR 7574, Chimie de la Matière Condensée de Paris (LCMCP), Collège de France, 11 Place Marcelin Berthelot, F-75231 Paris (France).

^c Univ Paris Diderot, Sorbonne Paris Cité, Interfaces, Traitements, Organisation et Dynamique des Systèmes (ITODYS), UMR 7086, CNRS, 15 Rue Jean-Antoine de Baïf, F-75205 Paris Cedex 13 (France).

Electronic Supplementary Information (ESI) available: See DOI: 10.1039/b000000x/

References

1. C. K. Kuo and P. X. Ma, *Biomaterials*, 2001, **22**, 511-521.
2. H. Zhang, E. Tumarkin, R. Peerani, Z. Nie, R. M. Sullan, G. C. Walker and E. Kumacheva, *J. Am. Chem. Soc.*, 2006, **128**, 12205-12210.
3. G. T. Franzesi, B. Ni, Y. Ling and A. Khademhosseini, *J. Am. Chem. Soc.*, 2006, **128**, 15064-15065.
4. D. W. Green, I. Leveque, D. Walsh, D. Howard, X. Yang, K. Partridge, S. Mann and R. O. C. Oreffo, *Adv. Funct. Mater.*, 2005, **15**, 917-923.
5. H. Kong, M. K. Smith and D. J. Mooney, *Biomaterials*, 2003, **24**, 4023-4029.
6. G. Orive, S. Ponce, R. M. Hernández, A. R. Gascón, M. Igartua and J. L. Pedraz, *Biomaterials*, 2002, **23**, 3825-3831.
7. A. D. Augst, H. J. Kong and D. J. Mooney, *Macromol Biosci*, 2006, **6**, 623-633.
8. R. Brayner, M.-J. Vaulay, F. Fiévet and T. Coradin, *Chem. Mater.*, 2007, **19**, 1190-1198.
9. P. Agulhon, S. Constant, B. Chiche, L. Lartigue, J. Larionova, F. Di Renzo and F. Quignard, *Catal. Today*, 2012, **189**, 49-54.
10. Y. Monakhova, P. Agulhon, F. Quignard, N. Tanchoux and D. Tichit, *Catal. Today*, 2012, **189**, 28-34.
11. F. Liu, L. D. Carlos, R. A. Ferreira, J. Rocha, M. C. Gaudino, M. Robitzer and F. Quignard, *Biomacromolecules*, 2008, **9**, 1945-1950.

12. A. Haug and O. Smidsrød, *Nature*, 1967, **215**, 757-757.
13. P. Agulhon, M. Robitzer, L. David and F. Quignard, *Biomacromolecules*, 2012, **13**, 215-220.
14. C. Karakasyan, M. Legros, S. Lack, F. Brunel, P. Maingault, G. Ducouret and D. Hourdet, *Biomacromolecules*, 2010, **11**, 2966-2975.
15. J. L. Mongar and A. Wassermann, *Journal of the Chemical Society*, 1952, 500-510.
16. I. L. Mongar and A. Wassermann, *Chemistry & Industry*, 1949, 27-27.
17. M. Perullini, M. M. Rivero, M. Jobbágy, A. Mentaberry and S. A. Bilmes, *J. Biotechnol.*, 2007, **127**, 542-548.
18. M. C. Gutiérrez, Z. Y. García-Carvajal, M. Jobbágy, F. Rubio, L. Yuste, F. Rojo, M. L. Ferrer and F. del Monte, *Adv. Funct. Mater.*, 2007, **17**, 3505-3513.
19. M. a. C. Gutiérrez, Z. Y. García-Carvajal, M. a. J. Hortigüela, L. Yuste, F. Rojo, M. a. L. Ferrer and F. del Monte, *J. Mater. Chem.*, 2007, **17**, 2992.
20. M. Perullini, M. Jobbágy, G. J. A. A. Soler-Illia and S. A. Bilmes, *Chem. Mater.*, 2005, **17**, 3806-3808.
21. Y. Ferro, M. Perullini, M. Jobbágy, S. A. Bilmes and C. Durrieu, *Sensors (Basel)*, 2012, **12**, 16879-16891.
22. M. Perullini, M. Jobbágy, N. Mouso, F. Forchiassin and S. A. Bilmes, *J. Mater. Chem.*, 2010, **20**, 6479.
23. B. H. A. Rehm, *Alginate: Biology and Applications*, Springer, 2009.
24. C. Sicard, M. Perullini, C. Spedalieri, T. Coradin, R. Brayner, J. Livage, M. Jobbágy and S. A. Bilmes, *Chem. Mater.*, 2011, **23**, 1374-1378.
25. M. Perullini, M. Jobbágy, S. A. Bilmes, I. L. Torriani and R. Candal, *J. Sol-Gel Sci. Technol.*, 2011, **59**, 174-180.
26. A. Coiffier, T. Coradin, C. Roux, O. M. M. Bouvet and J. Livage, *J. Mater. Chem.*, 2001, **11**, 2039-2044.
27. M. Perullini, M. Jobbágy, M. L. Japas and S. A. Bilmes, *J. Colloid Interface Sci.*, 2014, **425**, 91-95.
28. M. Perullini, Y. Ferro, C. Durrieu, M. Jobbágy and S. A. Bilmes, *J. Biotechnol.*, 2014.
29. A. Pannier, U. Soltmann, B. Soltmann, R. Altenburger and M. Schmitt-Jansen, *J. Mater. Chem. B*, 2014, **2**, 7896-7909.
30. C. Y. Hui, Y. Li and J. D. Brennan, *Chem. Mater.*, 2014, **26**, 1896-1904.
31. A. Leonard, P. Dandoy, E. Danloy, G. Leroux, C. F. Meunier, J. C. Rooke and B. L. Su, *Chem. Soc. Rev.*, 2011, **40**, 860-885.
32. C. Sicard, R. Brayner, J. Margueritat, M. Hémadi, A. Couté, C. Yéprémian, C. Djediat, J. Aubard, F. Fiévet, J. Livage and T. Coradin, *J. Mater. Chem.*, 2010, **20**, 9342.
33. V. Jaouen, R. Brayner, D. Lantiat, N. Steunou and T. Coradin, *Nanotechnology*, 2010, **21**, 185605.

Acid gelation of alginate allows the inclusion of living cultures within sol-gel silica hydrogels. The former bead spontaneously reverts into a liquid viable culture.

